KSCE Journal of Civil Engineering (2019) 23(5):2254-2262

DOI 10.1007/s12205-019-1268-7

Structural Engineering

pISSN 1226-7988, eISSN 1976-3808
www.springer.com/12205

Study of the Ultimate Bearing Capacity of Concrete-filled Steel Tube K-Joints

Kaizhong Xie*, Hongwei Wang, Jinhao Pang***, and Jianxi Zhou******

Received June 25, 2018/Revised 1st: September 6, 2018, 2nd: November 21, 2018/Accepted January 2, 2019/Published Online February 1, 2019

Abstract

To study the ultimate bearing capacity of Concrete-Filled Steel Tube (CFST) K-joints, theoretical analysis and numerical simulation methods were adopted. A finite element model of a K-joint was established and verified with test data. Based on this model, the failure modes of the K-joint were studied. The results showed that the load-displacement curves of CFST K-joints can be divided into three stages: an elastic stage, an elastic-plastic stage and a failure stage. There were two types of failure modes for K-joints: local buckling failure at the connection between a branch pipe and the main pipe due to compression and tearing failure at the connection between a branch pipe and the main pipe due to tensile forces. The factors that influence the ultimate bearing capacity of CFST K-joints were studied, and the results were as follows. The ultimate bearing capacity increased as the radius-thickness ratio of the main pipe, radius-thickness ratio of the branch pipes and gap between branch pipes decreased. Additionally, the ultimate bearing capacity of the CFST K-joints increased with increasing core concrete grade, outer diameter ratio and thickness ratio between the branch pipe and main pipe. As the angle between the axis of the branch pipe and the axis of the main pipe increased, the ultimate bearing capacity initially decreased and then increased. As the axial pressure level in the main pipe increased, the ultimate bearing capacity of the K-joint initially increased and then decreased. A positive linear correlation was observed between the growth coefficient of the ultimate bearing capacity and the scaling factor. Moreover, the ultimate bearing capacity of CFST K-joints can be significantly improved by using core concrete. Finally, formulas for the ultimate bearing capacity of K-joints under different failure modes were proposed, and the results provide a reference for the design of CFST arch bridges.

Keywords: *K-joint, concrete-filled steel tube, ultimate bearing capacity, failure mode, influencing factors*

1. Introduction

Compared to other bridge types, Concrete-Filled Steel Tube arch bridges (CFST arch bridges) have many advantages, such as their flowing shapes and long spans; therefore, CFST arch bridges have been widely used in practical engineering (Chen *et al*., 2017b). As a key part of a CFST arch bridge, K-joints influence the strength and stability of the bridge. Although the rapid development (Zheng *et al*., 2014; Zheng, 2016) of CFST structures has occurred, research on the failure mode and ultimate bearing capacity of K-joints is lacking and requires further investigation. Currently, there is a lack of experimental research on CFST K-joints. Sakai *et al*. (2004) conducted a static load and fatigue test of K-joints and noted that the fatigue strength of CFST K-joints was higher than that of steel tube K-joints. Chen and Huang (2009) performed ultimate bearing capacity comparison tests of CFST K-joints and steel tube K-joints and found that the failure mode of K-joints was related to the thickness of the branch pipes; additionally, they noted that using core concrete in the main pipes of CFST K-joints can significantly improve the ultimate bearing capacity and stiffness of K-joints (Huang and Chen, 2006; Chen and Huang, 2007). However, in these studies, the factors that influenced the ultimate bearing capacity of K-joints were not quantitatively investigated. Zheng (2011) studied the factors that influence the failure modes and ultimate bearing capacity of planar CFST K-joints based on a finite element simulation method; however, the finite element model lacked experimental data verification, and few factors were found to affect the ultimate bearing capacity of the K-shaped joints at relatively small levels. Huang *et al*. (2015) conducted a full-scale test of CFST K-joints and noted that the punching shear failure mode was a typical failure mode of CFST K-joints before branch pipe failure occurred. Additionally, the ultimate bearing capacity of CFST K-joints in punching shear failure mode was close to the ultimate bearing capacity based on the Eurocode 3 specification; however, this study did not include a quantitative analysis of the factors that affect the ultimate bearing capacity of K-shaped joints. In addition to commonly used single-wall CFST K-joints in CFST arch bridges, scholars have researched double-wall CFST K-joints. Hou *et al*. (2017) performed an ultimate bearing capacity experiment of twenty double-wall CFST K-joints and found that the local buckling of compression branch pipes was a

*Professor, College of Civil Engineering and Architecture, Guangxi University, Nanning 530004, China (E-mail: xiekaizhong@163.com)
**Ph.D. Student, College of Civil Engineering and Architecture, Guangxi University, Nanning 530004, China (Corresponding Author, E-mail: 779348631@qq.com)
***M.Sc. Student, College of Civil Engineering and Architecture, Guangxi University, Nanning 530004, China (E-mail: 278485499@qq.com)
****M.Sc. Student, College of Civil Engineering and Architecture, Guangxi University, Nanning 530004, China (E-mail: 136098954@qq.com)

typical failure mode associated with double-wall CFST K-joints. The ratio of the diameter of branch pipes to that of the main pipe had a considerable influence on the ultimate bearing capacity of the double-wall CFST K-joints, and a strength prediction method for double-wall CFST K-joints was presented. In addition, Chen *et al*. (2017a) studied the spatial effect of CFST KK-joints and noted that the spatial effect did not change the failure mode of the joints but reduced the bearing capacity to a certain extent. Wang *et al*. (2018) obtained the ultimate bearing capacity of K-joints under different failure modes. In summary, in previous research, few studies considered the factors that influence the ultimate bearing capacity of K-joints, and many studies were limited; for example, they lacked experimental verification for finite element modeling and did not consider all influential factors. Moreover, because the failure mode and stress mechanism of K-joints are complicated, modeling experiments have also had limitations, such as not fully considering all influential parameters and high experimental costs. Therefore, to study the ultimate bearing capacity of K-shaped joints and the associated influential factors, based on the ultimate bearing capacity experiment conducted by Chen and Huang (2009), finite element models of CFST K-joints and steel tube K-joints were established and validated. A theoretical analysis method and numerical simulation method were adopted to study the failure mode and ultimate bearing capacity of the CFST K-joints, and formulas for the ultimate bearing capacity of the CFST K-joints were proposed under different failure modes. The findings provide a reference for the design of CFST arch bridges.

2. An Overview of the Specimen

To quantitatively study the ultimate bearing capacity of concrete-filled steel tube K-joints and establish an accurate finite element model, the specimen parameter values are important. According to the structure of a typical concrete-filled, steel, tubular arch bridge used in practical projects, the parameters of the specimen were determined. A schematic diagram of a CFST K-joints is shown in Fig. 1, and a loading diagram of a CFST K-joint is shown in Fig. 2.

The specific parameters of the K-joint were as follows: *L*-length of main pipe, L = 2000 mm; *l*-length of branch pipe, l = 900 mm; *D*-outer diameter of main pipe, D = 510 mm; *d*-outside diameter of branch pipe, d = 219 mm; *T*-thickness of main pipe, T =10 mm; *t*-thickness of branch pipe; θ-angle between the main pipe axis and branch pipe axis, $\theta = 60^{o}$; and *g*-gap between two branches, g = 51 mm. The core concrete in main pipe was C40. The thickness of branch pipes differed based on two cases: t = 6 mm and t = 8 mm. The ratio of the branch pipe radius to the branch pipe thickness was $\gamma = d/(2t)$. The ratio of the main pipe radius to the main pipe thickness was $k = D/(3T)$. The ratio of the outer diameter of a branch pipe to the outer diameter of the main pipe was $w = d/D$. The ratio of the branch pipe thickness to the main pipe thickness was $\tau = t/T$.

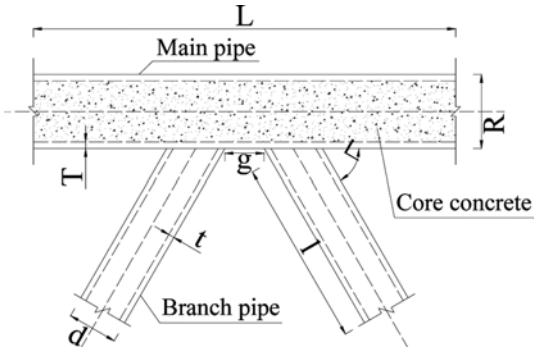

Fig. 1. Schematic Diagram of a CFST K-joint

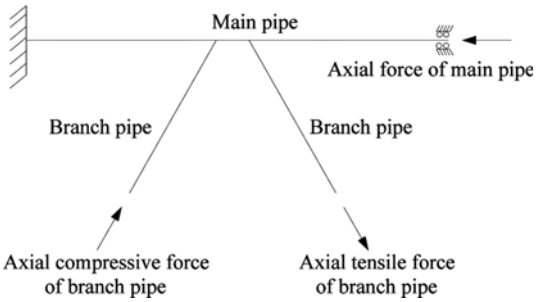

Fig. 2. Loading Diagram of a CFST K-joint

3. Finite Element Model

3.1 Model Overview

A 3D refined finite element model of a K-joint was established with ANSYS software. The contact between the steel tube and concrete was considered and stimulated by a contact unit. Additionally, geometric nonlinearity and material nonlinearity were considered. The basic objective was as follows. Considering the failure mode and ultimate bearing capacity of a K-joint, small deformation, small element rotation and large element strain will result in large error. In addition, these conditions do not agree with the actual conditions in practical applications; therefore, the K-joint deformation and element rotation were arbitrarily large during the analysis, and the element strain was very small. Because steel is an elastic-plastic material, if the plasticity is not considered, the ultimate bearing capacity of the K-joint will be inaccurately modeled, and the wrong failure modes may be obtained. Therefore, the steel pipe was an ideal elastic-plastic material. The effects of welds and welding residual stress were not considered. There is currently no good method of considering these influences, and further investigation is needed.

The steel tube was stimulated with the Solid92 unit. This unit includes a quadratic displacement function that is suitable for structural simulations of irregular shapes, and the unit includes plasticity, expansion, creep, stress tempering, large deformation and large strain functions. The concrete was simulated with the Solid65 unit. This unit can handle nonlinear material problems and simulate cracking in three orthogonal directions in concrete, as well as crushing, plastic deformation and creep. There were

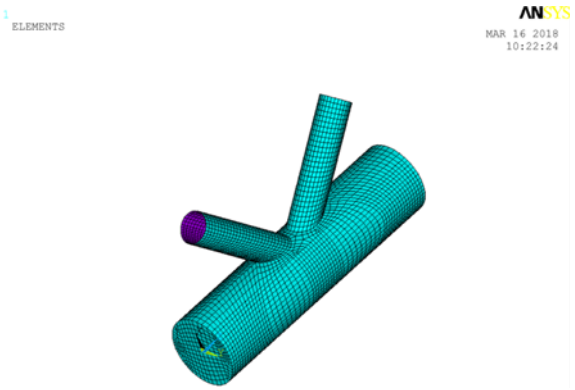

Fig. 3. Finite Element Model of the K-joint

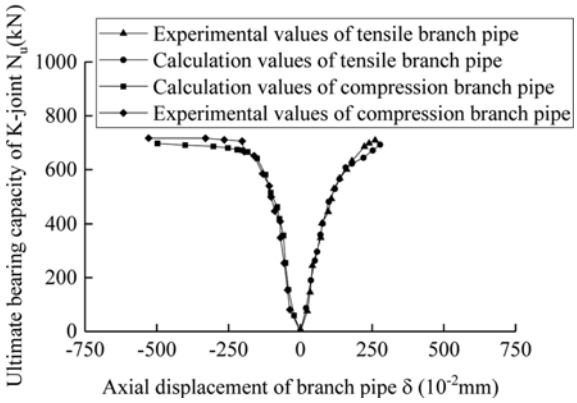

Fig. 4. Comparison Curves for Specimen CHSS-6

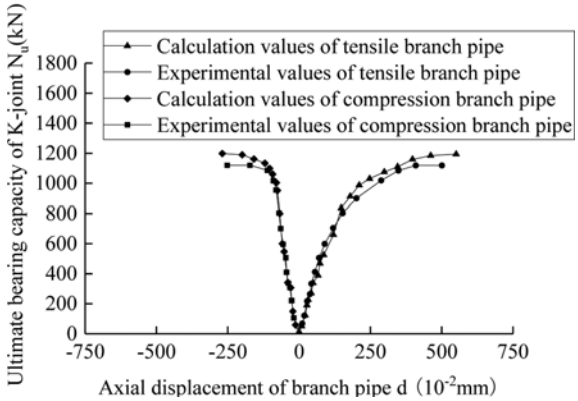

Fig. 5. Comparison Curves for Specimen CFST-6

22,116 units and 20,535 nodes in the finite element model. A bilinear isotropic elastic-plastic constituent relation was adopted for the steel tube material. Additionally, the yield strength f_y was 325 MPa, and the von Mises yield condition was used; specifically, when $\varepsilon < 0.0016$, $\sigma = E\varepsilon$, and when $\varepsilon > 0.0016$, $\sigma = f_y$. The constitutive relationship for core concrete proposed by Han (1997) was adopted. The Mohr-Coulomb yield criterion was adopted as the failure criterion because it is suitable for concrete compressed in three directions. One end of the main pipe was consolidated. The other end could only move in the direction of the main pipe. The finite element model of the K-joint is shown in Fig. 3.

3.2 Model Verification

To check the accuracy of CFST K-joint finite element model, based on ultimate bearing capacity experiment of the CFST K-joint conducted by Chen and Huang (2009), two steel tube K-joint members (CHSS-6 and CHSS-8) and two CFST K-joint members (CFST-6 and CFST-8) were compared and analyzed. The yield strength of the branch pipe with a thickness of 6 mm was 330 MPa, the ultimate strength was 485 MPa, the elongation was 21%, and the modulus of elasticity was 200 GPa. The yield strength of the branch pipe with a thickness of 8 mm was 325 MPa, the ultimate strength was 190 MPa, the elongation was 22%, and the modulus of elasticity was 200 GPa. The structural parameters of the components were given in section 2.

The upper end of the main pipe was fixed on a counterforce pedestal, and an axial force of 4,800 kN was applied at three levels during the CFST K-joint experiment. Moreover, an axial force of 2,500 kN was applied at two levels during the steel tube K-joint experiment. The load was constant, and axial tension and compression were simultaneously applied to the two branch pipes. The axial displacement of each branch pipe linearly increased based on an incremental step load of 20 kN. When deformation growth reached the nonlinear stage, the incremental step load was reduced to 10 kN. When deformation growth approached the damage stage, the incremental step load was reduced to 5 kN. When the steel pipe cracked or partially buckled, the jack was quickly unloaded, and the test was stopped. Comparison curves for specimen CHSS-6 are shown in Fig. 4, and comparison curves for specimen CFST-6 are shown in Fig. 5.

Table 1. Comparison of Ultimate Bearing Capacity for CFST K-joint

Specimen number	Experimental values obtained by Chen and Huang (2009) (kN)	Finite element calculation value (kN)	Relative deviation
CHSS-6	717	690	–3.77%
CHSS-8	719	702	–2.36%
CFST-6	1,115	1,196	7.26%
CFST-8	1,541	1,564	1.49%

For the ultimate bearing capacity of the CFST K-joint, experimental and theoretical values are shown in Table 1. A comparative analysis was conducted, and the load-deformation relationship curves obtained from theoretical analysis were in good agreement with the load-deformation curves obtained from experiments. For the ultimate bearing capacity of CHSS-6, CHSS-8, CFST-6 and CFST-8, the maximum relative deviation between experimental values and finite element-based values was 7.26%, with an average relative deviation of 3.72%. Thus, the finite element model provides high-accuracy results.

4. Failure Modes of K-joints

To align the numerical analysis with the experiment, CFST K-joints were loaded to 4,800 kN in three stages, and the steel tube K-joint was loaded to 2,500 kN in two stages. Then, the pressure in the main pipe was held constant, and equal-increment and synchronous pressure and tensile forces were applied to the two branch pipes until the K-joint failed and the ultimate bearing capacity declined. When the K-joint failed, the load corresponding to the minimum value of peak stress in the branch pipes was selected as the ultimate bearing capacity of the K-joint. During the calculation and analysis process, the thickness of each branch pipe was set to 2 mm, 4 mm, 6 mm, 8 mm and 10 mm, and each of these conditions was divided into two cases: 1) The main pipe was filled with concrete, and 2) the main pipe was not filled with concrete. The K-joint (K-3) with a thickness of 6 mm and CFST K-joint (K-C3) with a thickness of 6 mm are shown in Fig. 6 to illustrate the relationship between the axial displacement of the branch pipes and the ultimate bearing capacity of the K-joint.

Statistical analyses of the load-displacement curves of K-joints were conducted, and the conclusions are as follows:

1. The load-displacement curves obtained from the finite element model reproduced the outcomes of the experimental tests. These curves for the K-joint can be divided into three stages: an elastic stage, an elastic-plastic stage and a failure stage. The elastic-plastic characteristics of K-C3 and K-3 were compared within the same axial displacement range (0–250 mm) of the branch pipe. The displacement change caused by the same load change for the K-3 specimen was great than that for the K-C3 specimen. Additionally, the elastic-plastic characteristics of the K-joint with a main pipe not filled with concrete were more obvious than those for the joint with a main pipe filled with concrete.
2. The ultimate bearing capacity of the steel tube K-joint was 693.5 kN, and the ultimate bearing capacity of the concrete-filled steel tubular K-joint was 1,195.6 kN. Based on the same structural dimensions, the elastic-plastic characteristics and ultimate bearing capacity of the two K-shaped joints were considerably different, and they should be given additional attention.
3. The ultimate bearing capacity of the K-joint can be significantly improved by filling the main pipe with concrete, and this process can also change the failure mode of the K-joint. When the main pipe of the K-joint was not filled with concrete, the failure mode of the K-joint could be divided into two cases. In the first case, the main pipe was damaged by branch pipe compression and punching failure, and in the second case, the main pipe was damaged by tensile forces and the excessive deformation of the branch pipe. When main pipe of the K-joint was filled with concrete, the failure mode of the K-joint could be divided into two cases. In the first case, the branch pipe experienced local buckling failure due to compression, and this damage occurred at the connection between the branch pipe and main pipe. In the second case, tearing failure occurred at the connection between the branch pipe and main pipe due to tensile forces.
4. The thickness of the branch pipe influenced the failure mode of the K-joint. In the failure stage, when the thickness of the

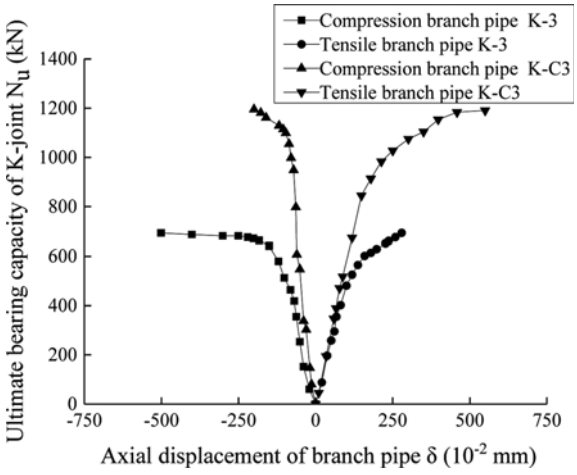

Fig. 6. Relationship between the Axial Displacement of the Branch Pipes and the Ultimate Bearing Capacity of the K-joint

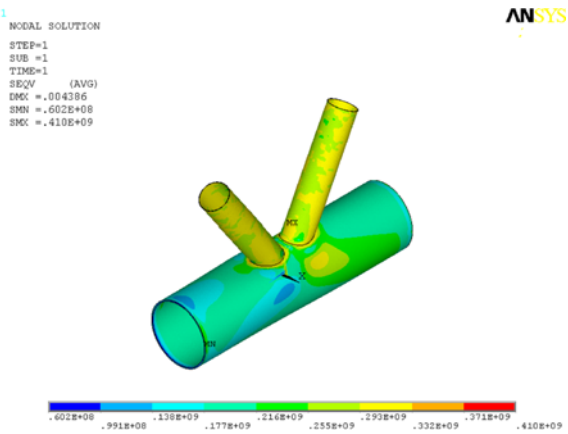

Fig. 7. Local Buckling Failure of the Branch Pipe due to Compression

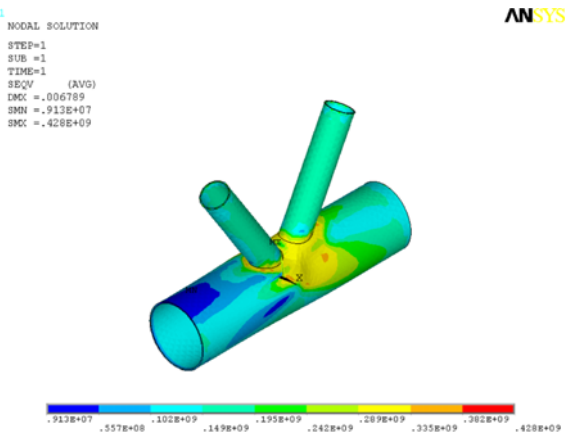

Fig. 8. Tearing Failure of the Main Pipe

branch pipe was less than or equal to 4 mm, local buckling failure occurred at the connection between the branch pipe and main pipe due to compression, as shown in Fig. 7. When the thickness of the branch pipe was greater than or equal to 6 mm, tearing failure occurred at the connection between the branch pipe and main pipe due to tensile forces, as shown in Fig. 8.

5. The influence of debonding between the steel pipe and concrete on the failure mode of the concrete-filled steel tubular K-joint is not considered in the calculation, and further research is needed. In addition, in recent years, some scholars have used internal welding studs to solve the problem of debonding. The influence of studs on the failure modes of CFSTs requires further investigation.

5. Factors that Influence the Ultimate Bearing Capacity

Based on the finite element model and failure modes of the K-joint, the following factors were found to influence the ultimate bearing capacity of the joint: the geometric size of the branch pipe and main pipe, the angle between the axis of the main pipe and the axis of the branch pipe, the gap between the two branch pipes, the grade of the core concrete, the axial pressure level in the main pipe, and the scaling coefficient of the K-joint.

5.1 Geometric Size

Geometric design is an important part of the development of concrete-filled steel tubular arch bridges. The design should be based on multiple calculations, and understanding the influence of geometric size changes on the ultimate bearing capacity of the K-joints helps to improve the design efficiency.

To study influence of geometric size on the ultimate bearing capacity of K-joints, values and ranges of parameters were selected as follows. The external diameter of the branch pipe d was divided into five cases: 319 mm, 269 mm, 219 mm, 169 mm and 119 mm. The thickness of the branch pipe t was divided into five cases: 2 mm, 4 mm, 6 mm, 8 mm and 10 mm. The thickness of the main pipe T was divided into five cases: 6 mm, 8 mm, 10 mm, 12 mm and 14 mm. The additional parameters associated with the K-joint are given in section 2. Only the ultimate bearing capacity values of the K-joint with d = 219 mm and D = 510 mm are shown in Table 2.

Table 2. Ultimate Bearing Capacity of the K-joint

t (mm)	Ultimate bearing capacity of K-joint (kN)				
	T = 6 mm	T = 8 mm	T = 10 mm	T = 12 mm	T = 14 mm
2	442	448	454	459	462
4	879	885	892	901	908
6	1,112	1,171	1,196	1,242	1,322
8	1,421	1,476	1,564	1,592	1,651
10	1,614	1,657	1,696	1,733	1,766

Various conclusions can be obtained from Table 2. Notably, as κ and γ decrease, the ultimate bearing capacity of the K-joint increases. Additionally, the influence of γ on the ultimate bearing capacity is greater than that of κ. Moreover, as ω and τ increase, the ultimate bearing capacity of the K-joint increases.

5.2 Angle between the Branch Pipe and Main Pipe and Gap between the Two Branch Pipes

Both the angle between the branch pipe and main pipe and the gap between the two branch pipes influence the ultimate bearing capacity of the K-joint. To quantitatively study the effects of these two factors, the parameters were divided into different levels.

The thickness of the branch pipe t was set to 6 mm and 8 mm, and the angle between the axis of the branch pipe and the axis of the main pipe θ was set to 30°, 45° and 60°. The gap between the two branch pipes g was divided into five cases: 0 mm, 25.5 mm, 51 mm, 76.5 mm and 102 mm. The additional parameters related to the K-joint are given in section 2. The effects of θ and g on the ultimate bearing capacity of the K-joint are shown in Table 3.

The conclusions obtained from Table 3 are as follows.

1. When thickness of the branch pipe t and the gap between the two branch pipes g were constant, as the angle θ between the axis of the branch pipe and that of the main pipe increased, the ultimate bearing capacity of the K-joint initially decreased and then increased. When the angle θ between the axis of the branch pipe and the axis of the main pipe increased from 30° to 45° and the thickness of the branch pipe was t = 6 mm, the ultimate bearing capacity of the K-joint decreased by 9.41% on average, and when t = 8 mm, the ultimate bearing capacity decreased by 9.73% on average. When the angle θ between the axis of the branch pipe and the axis of the main pipe increased from 45° to 60° and

Table 3. Influence of θ and g on the Ultimate Bearing Capacity of the K-joint

t (mm)	θ (°)	Ultimate bearing capacity of the K-joint (kN)				
		g = 0 mm	g = 25.5 mm	g = 51 mm	g = 76.5 mm	g = 102 mm
6	30	1,330	1,274	1,252	1,229	1,190
	45	1,197	1,163	1,128	1,117	1,079
	60	1,259	1,223	1,196	1,170	1,126
8	30	1,712	1,653	1,635	1,623	1,585
	45	1,548	1,505	1,485	1,452	1,420
	60	1,628	1,597	1,564	1,546	1,511

the thickness of the branch pipe was t = 6 mm, the ultimate bearing capacity of the K-joint decreased by 5.09% on average, and when t = 8 mm, the ultimate bearing capacity decreased by 5.90% on average. The calculation results indicate that the influence of the angle change on the ultimate bearing capacity of the K-joint was not uniform. This finding provides a reference for the design of concrete-filled steel tube arch bridges.

2. When the thickness of the branch pipe t and the angle θ between axis of the branch pipe and that of the main pipe were constant, as the gap g between the two branch pipes increased, the ultimate bearing capacity of the K-joint decreased. When, the gap g between the two branch pipes increased from 0 mm to 102 mm and the thickness of the branch pipe was t = 6 mm, the ultimate bearing capacity of the K-joint decreased by 10.32% on average, and when t = 8 mm, the ultimate bearing capacity decreased by 7.62% on average.

5.3 Core Concrete Grade

Core concrete is an important part of a concrete-filled steel tube structure, and it has a considerable influence on concrete-filled steel tube K-joints. To study the influence of core concrete changes on the K-joint, the grade of core concrete was divided into five classes: C20, C30, C40, C50 and C60. The influence of the core concrete on the ultimate bearing capacity of the K-joint is shown in Table 4.

The ultimate bearing capacity of the K-joint can be significantly improved by using core concrete. When the thickness of the branch pipe was t = 6 mm, the ultimate bearing capacity of the K-joint improved by 53.19%, and when t = 8 mm, the ultimate bearing capacity improved by 91.48%. The ultimate bearing capacity of the K-joint increased with increasing core concrete grade, and the increasing trend gradually slowed. When the thickness of the branch pipe was t = 6 mm and the core concrete grade changed from C20 to C60, the ultimate bearing capacity of the K-joint increased by 18.35%, and when t = 8 mm the core concrete grade changed from C20 to C60, the ultimate bearing capacity increased by 18.92%.

According to the calculation results, as the core concrete grade increased, the ultimate bearing capacity of the K-joint increased and gradually stabilized. The bearing capacity of the concrete-filled steel tube is mainly influenced by the type of steel pipe, type of concrete and the interactions between the steel and concrete. When the core concrete strength increased and the steel pipe strength was constant, the stable ultimate bearing capacity of the K-joint indicates that the confining effect of the steel tube is small. Therefore, in the design stage of concrete-filled steel tubular arch bridges, an excessively high core concrete grade will not significantly improve the performance of the CFSTs and will increase the project costs. Generally, the core concrete grade should match the thickness of the steel tube.

5.4 Axial Pressure Level in the Main Pipe

The axial pressure level in the main pipe was defined as the ratio between the applied axial pressure and the ultimate bearing capacity of the main pipe. The ultimate bearing capacity of the main pipe N_u was calculated using the equation proposed by Cai *et al*. (1984) as follows:

$$N_u = f_c A_c (1 + \theta + \sqrt{\theta}) \quad (1)$$

where f_c- is the compressional strength of the concrete without a lateral pressure, A_c is the area of the core concrete, and θ is the confinement coefficient. The axial pressure level in the main pipe was divided into six classes: 0.3, 0.4, 0.5, 0.6, 0.7 and 0.8. The influence of the axial pressure level in the main pipe on the ultimate bearing capacity is shown in Table 5.

The ultimate bearing capacity of the K-joint initially increased and then decreased as the axial pressure level in the main pipe increased. When, the thickness of the branch pipe was t = 6 mm and the axial pressure level in the main pipe increased from 0.3 to 0.5, the ultimate bearing capacity of the K-joint increased by 7.07%. When the axial pressure level in the main pipe increased from 0.5 to 0.8, the ultimate bearing capacity of the K-joint increased by 3.60%. When the thickness of the branch pipe was t = 8 mm and the axial pressure level in the main pipe increased from 0.3 to 0.5, the ultimate bearing capacity of the K-joint increased by 5.11%. Additionally, when the axial pressure level in the main pipe increased from 0.5 to 0.8, the ultimate bearing capacity of the K-joint increased by 1.92%.

5.5 Scaling Coefficient of the K-joint

The scaling factor is an important variable that affects the ultimate bearing capacity of K-joints. To quantitatively study the influence of this factor on the ultimate bearing capacity of the modeled K-joint, the coefficient ζ values were divided into five

Table 4. Influence of the Core Concrete Grade on the Ultimate Bearing Capacity of the K-joint

Grade of the core concrete		0	C20	C30	C40	C50	C60
Ultimate bearing capacity of the K-joint (kN)	t = 6 mm	690	1,057	1,139	1,196	1,228	1,251
	t = 8 mm	704	1,348	1,475	1,564	1,589	1,603

Table 5. Influence of the Pressure Level in the Main Pipe on the Ultimate Bearing Capacity of the K-joint

Pressure level in the main pipe		0.3	0.4	0.5	0.6	0.7	0.8
Ultimate bearing capacity of the K-joint (kN)	t = 6 mm	1,117	1,159	1,196	1,184	1,173	1,153
	t = 8 mm	1,488	1,526	1,564	1,555	1,546	1,534

Table 6. Scaling Parameters and Bearing Capacity of the K-joint

Specimen number	d (mm)	t (mm)	l (mm)	D (mm)	T (mm)	L (mm)	g (mm)	ζ	Calculated value of the ultimate bearing capacity (kN)	ρ
KSF-4	87.6	3.2	360.0	204.0	4.0	800.0	20.4	0.4	357	0.2
KSF-3	131.4	4.8	540.0	306.0	6.0	1,200.0	30.6	0.6	775	0.5
KSF-2	175.2	6.4	720.0	408.0	8.0	1,600.0	40.8	0.8	1,157	0.7
KSF-1	219.0	8.0	900.0	510.0	10.0	2,000.0	51.0	1.0	1,564	1.0
KSF-5	262.8	9.6	1,080.0	612.0	12.0	2,400.0	61.2	1.2	1,982	1.3

cases: 0.4, 0.6, 0.8, 1.0 and 1.2. In actual engineering, the value for a specific grade may not be reached, and the five cases are mainly to illustrate the influence of the scaling coefficient on the ultimate bearing capacity of the K-joint. The ultimate bearing capacity of the scaled K-joint was divided by the ultimate bearing capacity of the unscaled K-joint to obtain the growth coefficient ρ of the ultimate bearing capacity. The calculation results are shown in Table 6. Notably, the growth coefficient of the ultimate bearing capacity ρ and scaling coefficient ζ display a linear positive growth trend. Moreover, the rate of variation of the growth coefficient of the ultimate bearing capacity ρ is greater than that of the scaling coefficient ζ.

6. Ultimate Bearing Capacity Formulas for K-joints

Based on failure modes of K-joints and the factors that influence the ultimate bearing capacity of K-joints, formulas for the ultimate bearing capacity were derived for different failure modes.

6.1 Local Buckling of the Branch Pipe at the Joint Position due to Compression

The local buckling of the branch pipe at the joint position due to compression is a typical stable failure for a compressional member. In this case, if the thickness of the branch pipe is less than or equal to the limit thickness, local buckling failure can occur at the joint position. When the branch pipe is compressed, the internal force on the branch pipe exceeds the yield strength of the steel as follows:

$$N_{cu} = \varphi_c f_y A_c = \varphi_c f_y \times (\frac{\pi}{4} d^2 - \frac{\pi}{4}(d-2t)^2) = \pi \varphi_c f_y t(d-t) \quad (2)$$

where N_{cu} is the ultimate bearing capacity of the K-joint, A_c is the cross-sectional area of the branch pipe under compression, f_y is the yield strength of the branch pipe under compression, t is the thickness of the branch pipe under compression, d is the outer diameter of the branch pipe, and φ_c represents the factors that influence pipe stability under compression.

6.2 Tearing Failure of the Main Pipe at the Joint Position with a Branch Pipe under Tensile Forces

The tearing failure of the main pipe at the joint position with a branch pipe under tensile forces is a typical effective width failure related to the branch pipe. If the thickness of the branch pipe is larger than the limit thickness, local buckling failure can occur in the branch pipe. When branch pipe is pulled, the internal force on the main pipe at the joint position exceeds the yield strength of the steel. In this case, the failure of a circular CFST K-joint is more complex than that of a rectangular CFST K-joint, and it was difficult to establish an effective equation for the branch pipe. The effective width of the branch pipe was specified based on technical standards for rectangular CFST structures as follows:

$$b_e = \frac{10}{D/T}\frac{T}{t} d \le d \quad (3)$$

The ultimate bearing capacity equation for the branch pipe under tensile forces was derived from Packer (1995) as follows:

$$N_{u2} = f_y t(2.5d - 4t + b_e) \quad (4)$$

Based on Eq. (4), the modification coefficient ϕ_t of the ultimate bearing capacity of a circular CFST K-joint was introduced. This variable is related to the ratio τ of the branch pipe thickness to the main pipe thickness. When τ < 1.0, the finite element model values were slightly smaller than those from Eq. (4). Additionally, when $\tau \ge 1.0$, the finite element model values were slightly larger than those from Eq. (4). However, all deviations were all less than 10%, and $\phi_t = 0.9$. The following equation was obtained from Eq. (4):

$$N_{tu} = \varphi_t f_y t(2.5d - 4t + b_e) = \varphi_t f_y t(2.5d - 4t + 10T^2 d/Dt) \quad (5)$$

where f_y is the yield strength of the steel pipe, D is the external diameter of the main pipe, T is the thickness of the main pipe, d is the external diameter of the branch pipe under tensile forces, t is the thickness of the branch pipe under compression, b_e is the effective width of the branch pipe under tensile forces ($b_e \le d$), and ϕ_t is a correction factor. When $t = t/T$<1.0, ϕ_t = 1.0, and when $\tau = t/T \ge 1.0$, f_t = 0.9.

6.3 Accuracy Verification of the Ultimate Bearing Capacity Formula

The K-joint was analyzed based on the proposed formula for the ultimate bearing capacity. The length of the branch pipe l was 900 mm, the external diameter of the branch pipe d was 219 mm, the length of the main pipe L was 2,000 mm, the external diameter of the main pipe D was 510 mm, the angle between the axis of the branch pipe and the axis of the main pipe θ was 60°, the gap between the two branch pipes g was 51 mm, and the grade of the core concrete was C40. The thickness of the branch

Table 7. Comparison of the Ultimate Bearing Capacity Values of the K-joint

Specimen number	t (mm)	T (mm)	Failure mode	N_c (kN)	N_f (kN)	N_c/N_f
K3-11	2.0	6.0	Compression in the branch pipe	425	442	0.96
K3-21	4.0	6.0	Compression in the branch pipe	841	879	0.96
K3-31	6.0	6.0	Tensile forces in the branch pipe	1,071	1,112	0.96
K3-41	8.0	6.0	Tensile forces in the branch pipe	1,391	1,421	0.98
K3-51	10.0	6.0	Tensile forces in the branch pipe	1,530	1,614	0.95
K3-12	2.0	8.0	Compression in the branch pipe	425	448	0.95
K3-22	4.0	8.0	Compression in the branch pipe	841	885	0.95
K3-32	6.0	8.0	Tensile forces in the branch pipe	1,110	1,171	0.95
K3-42	8.0	8.0	Tensile forces in the branch pipe	1,430	1,476	0.97
K3-52	10.0	8.0	Tensile forces in the branch pipe	1,565	1,657	0.94
K3-13	2.0	10.0	Compression in the branch pipe	425	454	0.94
K3-23	4.0	10.0	Compression in the branch pipe	841	892	0.94
K3-33	6.0	10.0	Tensile forces in the branch pipe	1,160	1,196	0.97
K3-43	8.0	10.0	Tensile forces in the branch pipe	1,480	1,564	0.95
K3-53	10.0	10.0	Tensile forces in the branch pipe	1,610	1,696	0.95
K3-14	2.0	12.0	Compression in the branch pipe	425	459	0.93
K3-24	4.0	12.0	Compression in the branch pipe	841	901	0.93
K3-34	6.0	12.0	Tensile forces in the branch pipe	1,222	1,242	0.98
K3-44	8.0	12.0	Tensile forces in the branch pipe	1,541	1,592	0.97
K3-54	10.0	12.0	Tensile forces in the branch pipe	1,665	1,733	0.96

pipe t was divided into five cases: 2 mm, 4 mm, 6 mm, 8 mm and 10 mm. The thickness of the main pipe T was divided into four cases: 6 mm, 8 mm, 10 mm and 12 mm. A comparison between N_c values calculated using the derived formula and N_f values from the finite element model is shown in Table 7.

The calculation results were analyzed, and the values calculated based on the proposed equation were slightly smaller than those from finite element analysis however, the deviation was less than 8%. Overall, the values from the proposed equation are considered safe estimates. Moreover, based on the statistics of the finite element calculation results, when the thickness of each branch pipe $t \leq 4$ mm, Eq. (2) should be used to calculate the ultimate bearing capacity of CFST K-joints. In addition, when the thickness of each branch pipe $t > 4$ mm, Eq. (5) should be used to calculate the ultimate bearing capacity of CFST K-joints.

7. Conclusions

A theoretical analysis method and numerical simulation method were adopted to study the failure mode and ultimate bearing capacity of CFST K-joints. A finite element model of a CFST K-joint was established with ANSYS software and verified based on experimental results. Using this finite element model of a K-joint, the failure modes of the join and the factors that influence the ultimate bearing capacity of K-joints were studied. The following important conclusions were drawn from the results.

1. As the radius-thickness ratio of the main pipe κ and the radius-thickness ratio of the branch pipe γ decreased, the ultimate bearing capacity of the K-joint increased. The influence of γ was larger than that of κ. The ultimate bearing capacity of the K-joint increased as the external diameter ratio ω between the branch pipe and main pipe and the thickness ratio τ between the branch pipe and main pipe increased.
2. As the angle between the axis of the branch pipe and the axis of the main pipe increased, the ultimate bearing capacity of the K-joint initially decreased and then increased. When the axial pressure level in the main pipe was approximately 0.5, the ultimate bearing capacity of the K-joint peaked. As the gap between the two branch pipes increased, the ultimate bearing capacity of the K-joint decreased.
3. The ultimate bearing capacity of CFST K-joints can be significantly improved by filling the main pipe with core concrete. As the core concrete grade increased, the ultimate bearing capacity of the K-joint increased and eventually stabilized.
4. As the axial pressure level in the main pipe of the K-joint increased, the ultimate bearing capacity of the K-joint initially increased and then decreased. Additionally, when the axial pressure level in the main pipe was approximately 0.5, the ultimate bearing capacity of the K-joint peaked. A linear positive correlation was observed between the growth coefficient of the ultimate bearing capacity and the scaling factor. The rate of variation in the growth coefficient of the ultimate bearing capacity was larger than that of the scaling factor.

Finally, formulas for the ultimate bearing capacity of K-joints under different failure modes were proposed, and the findings provide a reference for the design of CFST arch bridges.

Acknowledgements

XIE thanks the National Natural Science Foundation of China

(Nos. 51868007, 51068001 and 51368005), the Systematic Project of Guangxi Key Laboratory of Disaster Prevention and Structural Safety (2012ZDX04) and the Scientific Research Foundation of Guangxi University (No. XBZ100762).

References

Cai, S. H. and Jiao, Z. S. (1984). "Behavior and ultimate strength of short concrete-filled steel tubular columns." *Journal of Building Structures*, No. 6, pp. 13-29.

Chen, B. C. and Huang, W. J. (2007). "Experimental research on ultimate load carrying capacity of truss girders made with circular tubes." *Journal of Building Structures*, Vol. 28, No. 3, pp. 31-36, DOI: 10.14006/j.jzjgxb.2007.03.005.

Chen, B. C. and Huang, W. J. (2009). "Experimental study on ultimate bearing capacity of CFST directly-welded K-joints." *China Civil Engineering Journal*, Vol. 42, No. 12, pp. 91-98, DOI: 10.15951/j.tmgcxb.2009.12.017.

Chen, J., Sun, W. J., and Nie, J. G. (2017a). "Study on spatial effect of concrete-filled steel tubular KK-joints." *Journal of Building Structures*, Vol. 38, No. S1, pp. 402-408, DOI: 10.14006/j.jzjgxb.2017.S1.056.

Chen, B. C., Wei, J. G., Zhou, J., and Liu, J. P. (2017b). "Application of concrete-filled steel tube arch bridges in China: Current status and prospects." *China Civil Engineering Journal*, Vol. 50, No. 6, pp. 50-61, DOI: 10.15951/j.tmgcxb.2017.06.006.

Han, L. H. (1997). "Theoretical analysis and experimental researches for the behaviors of high strength concrete filled steel tubes subjected to axial compression." *Industrial Construction*, Vol. 27, No. 11, pp. 39-44, DOI: 10.13204/j.gyjz1997.11.010.

Hou, C. and Han, L. H. (2017). "Analytical behavior of CFDST chord to CHS brace composite K-joints." *Journal of Constructional Steel Research*, Vol. 128, No. 2017, pp. 618-632, DOI: 10.1016/j.jcsr.2016.09.027.

Hou, C., Han, L. H., and Mu, T. M. (2017). "Behaviors of CFDST chord to CHS brace composite K-joints: Experiments." *Journal of Constructional Steel Research*, Vol. 135, No. 2017, pp. 97-109, DOI: 10.1016/j.jcsr.2017.04.015.

Huang, W. J. and Chen, B. C. (2006). "Experimental research on concrete filled steel tube truss girder under bending." *Journal of Architecture and Civil Engineering*, Vol. 23, No. 1, pp. 29-33, DOI: 10.3321/j.issn:1673-2049.2006.01.005.

Huang, W. J., Fenu, L., Chen, B. C., and Briseghella, B. (2015). "Experimental study on K-joints of concrete-filled steel tubular truss structures." *Journal of Constructional Steel Research*, Vol. 107, pp. 182-193, DOI: 10.1016/j.jcsr.2015.01.023.

Packer, J. A. (1995). "Concrete-filled HSS connections." *Journal of Structural Engineering*, Vol. 121, No. 3, pp. 458-467, DOI: 10.1061/(ASCE)0733-9445(1995)121:3(458).

Sakai. Y., Hosaka, T., Isoe, T., Ichikawa, A., and Mitsuki, K. (2004). "Experiments on concrete filled and reinforced tubular K-joints of truss girder." *Journal of Constructional Steel Research*, Vol. 60, Nos. 3-5, pp. 683-699, DOI: 10.1016/S0143-974X(03)00136-6.

Wang, J. F., Deng, Q., and Xing, W. B. (2018). "Calculation method of the ultimate bearing capacity for circular CFST Truss K-joints." *Progress in Steel Building Structures*, Vol. 20, No. 2, pp. 44-52, DOI: 10.13969/j.cnki.cn31-1893.2018.02.006.

Zheng, L. Q. (2011). "Mechanical property analysis of concrete-filled circular steel tubular K-joints of truss." *Steel Construction*, Vol. 26, No. 11, pp. 20-23, DOI: 10.3969/j.issn.1007-9963.2011.11.005.

Zheng, J. L. (2016). "New development technology of large-span reinforced concrete arch bridges in China." *Journal of Chongqing Jiaotong University (Natural Science)*, Vol. 35, No. S1, pp. 8-11, DOI: 10.3969/j.issn.1674-0696.2016.sup1.02.

Zheng, J. L., Wang, J. J., Mou, T. M., Feng, Z., Han, Y., and Qin, D. Y. (2014). "Feasibility study on design and construction of concrete filled steel tubular arch bridge with a span of 700 m." *Engineering Sciences*, Vol. 16, No. 8, pp. 33-37, DOI: 10.3969/j.issn.1009-1742.2014.08.004.